DRYING OF POROUS PARTICLES WETTED WITH A LIQUID MIXTURE IN A FLUIDIZED BED WITH HEATED WALLS

G. AFRANE M.S. P-G. Dip.
Department of Chemical Engineering
University of Science and Technology,
Kumasi, Ghana

J. SCHWARZBACH Ph.D.
Institute of Thermal Processes
University of Karlsruhe, West Germany.

ABSTRACT

Although water is often the only solvent used, there are several important industrial applications where a mixture of liquids with different volatilities are involved. In such cases not only the drying rate but also the variation of the compostion of the liquid contained in the solids with the moisture content of the particles is of interest. This could reveal whether or not a partial preferential removal of one component or the other is possible in the course of the drying. In this study a 1m long, 0.2m diameter fluidized bed with heated walls and various mixtures of iso-propanol and water was used. Results obtained indicate that mild drying conditions promote more selectivity since the process-controlling liquid-side mass transfer resistance, increases with the severity of drying.

Keywords: Selectivity, heat and mass transfer coefficients, fluidization, drying.

INTRODUCTION

Due to the excellent contact obtained between the vapour-carrying gas stream (which is normally air) and the solids, fluidized beds are extensively used for drying granulated products and grains. Normally the gas stream is heated prior to its entry into the fluidised bed. However drying can also be carried out where heated walls or heating elements immersed in the bed are used. Where the two modes of contact are combined, the much increased heat transfer coefficients resulting can lead to a reduction in dryer size.

In this work a fluidized bed with heated walls and an iso-propanol-water mixture was used with the objective of studying the effect of the mode of heat transfer and operating parameters on selectivity. By selectivity it is meant the preferential removal of one of the component from the liquid phase. Normally the component of highest volatility constitutes the largest fraction in the escaping vapour at the start of drying. However the interaction of capillarity of the porous material and the gas-and liquid-side resistances can lead to a different result.

A 1m long hollow copper unit with a diameter of 0.2m long was used. The first systematic study of the evaporation of a binary mixture from a free liquid surface was reported by Sklarenko and Baranajew (1,2) and Lewis and Squires (3). In recent times a series of work has been done with different modes of drying by Schlunder and co-workers. Work has been reported on convective drying of porous particles (4); vacuum contact drying of catalysts pellets (5); and fluidized bed drying of porous particles all wetted with binary mixtures (6).

THEORY

Depending on the initial moisture content and the nature of the wetted material the

drying rate curves of solids can be roughly divided into three segments. These are the constant rate period, during which unbound moisture is dried off and which terminates at the critical moisture content; and the first and second falling rate periods when bound moisture is removed. Selectivity in the course of drying mixture-wetted solids is controlled by a complex, combination of several factors. These are the extent of mixing and sorption effects, capillarity in pores, thermodynamic equilibrium between the gas and liquid phases and mass transfer in the dried, partially dried and wet pores. To simplify the mathematical treatment of the process, those factors of minor influence are conveniently neglected. The treatment is divided into four sections:

. sorption and mixing effects
. mass transfer in the pores of the particles
. heat and mass transfer in the fluidized bed, and
. heat transfer between heated wall and bed.

2.1. Effect of Sorption, Mixing and Capillarity

At the beginning of the process when the liquid forms a continuous phase on the surface of the particles as well as in the pores, interaction between the liquid and the solid is unimportant. Later when the liquid becomes a discontinuous phase, sorption effects can increase in importance depending on whether the solid is hygroscopic or not. Thurner and Schlunder (7) have measured sorption isotherms between non-hygroscopic brick and hygroscopic paper as the solids, and water and isopropanol as liquids. The results show that even at low moisture contents when they begin to enter into the picture, sorption effects have very little influence on selectivity.

Experiments conducted by Fitzgerald (8) with tracer materials and beds without tubes indicate good gas-solid mixing. For superficial velocities between 1.5 and 3.4 m/s overall mixing times of between 50 and 10s were reported for a 1m square bed. Superficial velocities involved in this work was between 1.1 and 2.1 m/s and drying times ranged from 300 to 2000s. Therefore given the smaller size of the bed (0.03m square) thorough mixing of the bed is expected. Based on this assumption, temperatures and concentrations measured are taken as representative of the entire bed.

At the initial stage of the drying when the liquid forms a continuous phase, it is transported to the surface of the particles by capillary action. The capillary transport is due to the surface tension of the fluid at the surface of the particles. This creates a pressure gradient in the pores. As the drying progresses the moisture content of the particles reduces to the critical moisture content, after which the drying front recedes into the particle. The shrinking core model, which was originally employed to describe gas-solid reactions, has also been applied successfully to described drying in porous particles (9, 10). It assumes that drying takes place only at the drying front and that after the critical moisture content is reached the moisture content stays at this value till the end of the process. The drying rate drops, however since the additional resistance introduced by the dried outer shell increases with time (fig. 1). The results of such a model compared to some experimental values are shown in figure 2. This is a plot of mole fraction versus the relative moisture content in the particle.

2.2. Mass Transfer in the Particle Pores

Selectivity in the evaporation of mixture systems has been defined as (4):

$$S_1 = \hat{Y}_1 - \tilde{x}_1 \qquad (1)$$

where for a binary system

$$\hat{Y}_1 = \frac{\dot{N}_1}{\dot{N}_1 + \dot{N}_2} = \frac{\tilde{Y}_1^*}{\tilde{Y}_1^* + \tilde{Y}_2^*} \qquad (2)$$

and

$$x_1 = \frac{N_1}{N_1 + N_2} \qquad (3)$$

S_1 can be positive, negative or zero, indicating removal or retention of component 1 or no change in the initial

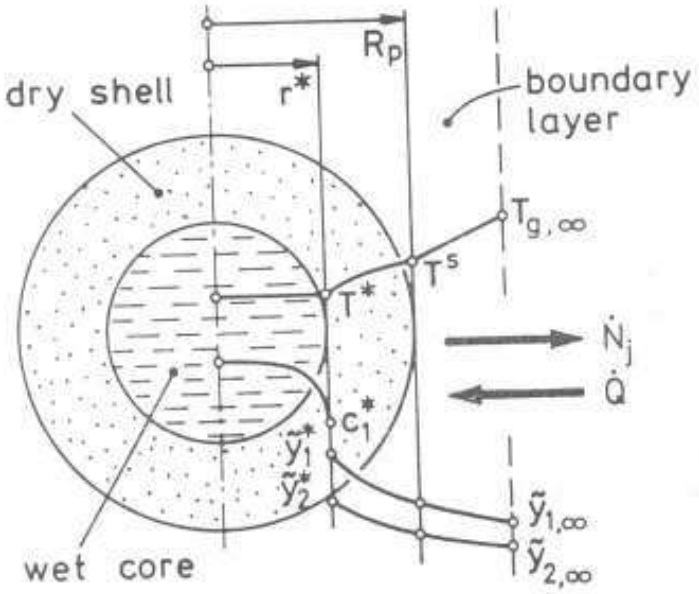

Fig. 1. The shrinking core model.

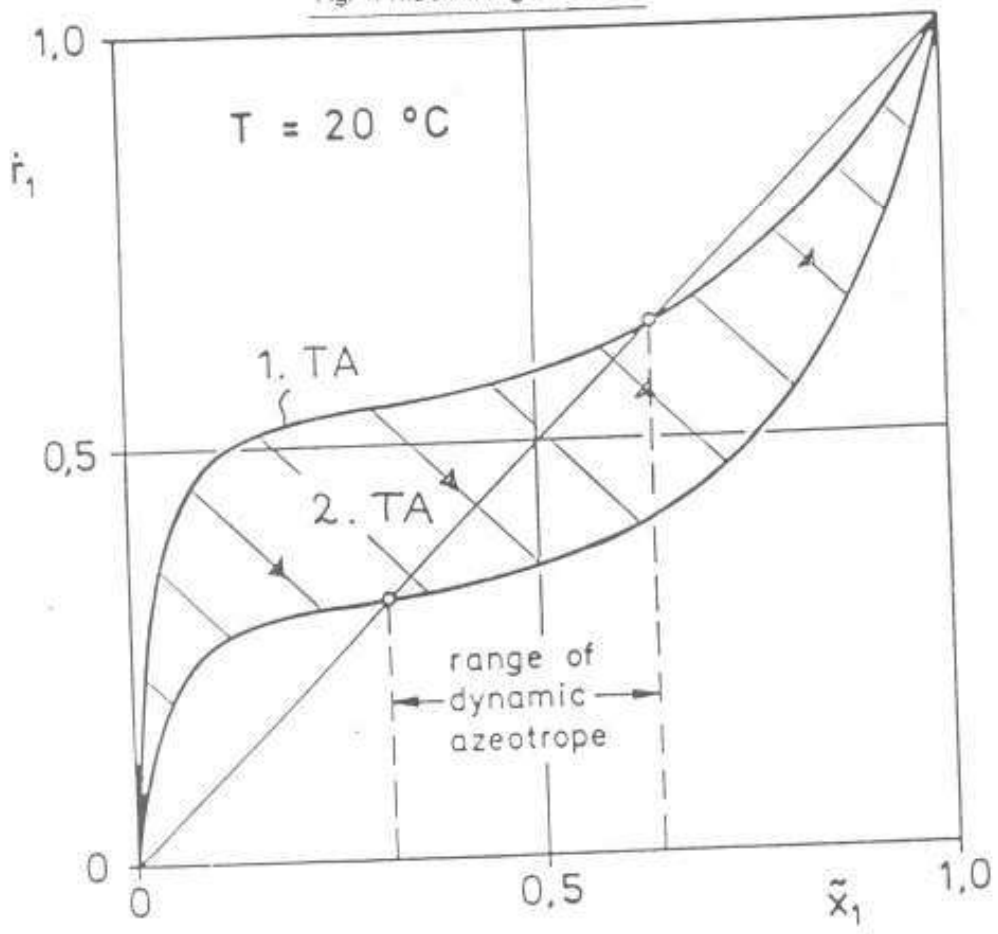

Fig. 2. The limiting cases of selectivity.

composition, respectively. The equilibrium diagram for isopropanol-water mixture shows a dynamic azeotrope between mole fractions 0.63 at the start and 0.32 at the end of the drying (fig.2).

Considering equation (1) and figure 2, the maximum selectivity will be obtained from curve 1 and the minimum from curve 2. Curve 1 represents the case where equilibrium between the liquid and the bed gas controls the drying. By the time of curve 2 the liquid does not form a continuous phase in the porous solid any more and the resistance due to the dried and partially dried solid interfere. The process is now diffusion controlled.

By a combination of volume balance, molar flux balance around a spherical particle and the continuity equation the variation of the concentration of the liquid with time in the pores during drying can be calculated (6). This is used in developing the concentration profiles given in the composition curves of fig. 3.

2.3. Heat and Mass Transfer in the Fluidized Bed

Heat and mass transfer coefficients between the drying front and the gas are calculated on the basis of the plug flow model for the gas flow through the bed. It is assumed that the bed is ideally mixed and that there is no back-mixing of the gas. The mass balance expression

$$\dot{N}_g \, d\tilde{Y}_i = \dot{n}_1 dA \qquad (4)$$

and the kinetic expression

$$\dot{n}_1 = n_g K_{i,g} (\tilde{Y}_i^* - \tilde{Y}_i) \qquad (5)$$

gives $$\frac{(\tilde{Y}_i^* - \tilde{Y}_i)_{out}}{(\tilde{Y}_i^* - \tilde{Y}_i)_{in}} = e^{-NTU_i^I} \qquad (6)$$

where $$\tilde{Y}_i = \frac{Y_i}{1 - Y_1 - Y_2} \qquad (7)$$

and $$NTU_i^I = \frac{A_b \, n_g \, K_{i,g}}{\dot{N}_g} \qquad (8)$$

NTU's are the number of transfer units. The $\tilde{Y}_i$'s are determined from vapour-liquid equilibrium data while the Y_i's are measured directly. Similar expressions are obtained for heat transfer.

$$\frac{T_{g,out} - T_g}{T_{g,out} - T_p} \ln = e^{-NTU_t} \qquad (9)$$

where $$NTU_i^I = \frac{A_g \, \alpha_g}{C_{pg} \dot{M}_g} \qquad (10)$$

The NTU's can be expressed in terms of Sherwood and Nusselt numbers as:

$$Sh_{pi} = \frac{1}{6} \frac{(1 - \varepsilon_b) d_p}{H_{b,o}} = NTU_i Pe_{pi} \qquad (11)$$

where Pe_{pi} the Peclet number is given by

$$Pe_{pi} = \frac{u_g \, d_p}{D_{ig}} = Re_p Sc_i \qquad (12)$$

Similarly

$$NTU_t = 6 \frac{H_{b,o}}{(1-\varepsilon_{b,o}) d_p} \frac{Nu_p}{Re_p} \qquad (13)$$

A plot of Sh_{pi} versus Re_p from various sources is shown in fig. 5. The data were obtained from equipment of different sizes and from different systems. They show that Sh_{pi} is dependent not only on Re_p and Sc_i but also on various system parameters like diameter of bed, distributor type, bed height etc. Thus it is recommendable to measure the mass transfer coefficient for the specific equipment concerned.

The reduced NTU value for mass transfer during the falling rate period is given by:

$$NTU_i^{II} = \frac{NTU_i^I}{1 + 0.5 Bi_i \left[\frac{R_p}{r^*} - 1 \right]} \qquad (14)$$

where Bi, the Biot number is defined as:

$$Bi_i = \frac{K_{i,g} \, d_p}{D_{i,g}} \frac{\mu_p}{\varepsilon_p} \qquad (15)$$

- material: alumina-silicate
- liquid: 2-propanol (1)-water
- gas inlet temperature: 100°C
- mean particle diameter: 0.61 mm
- initial bed height: 15 cm

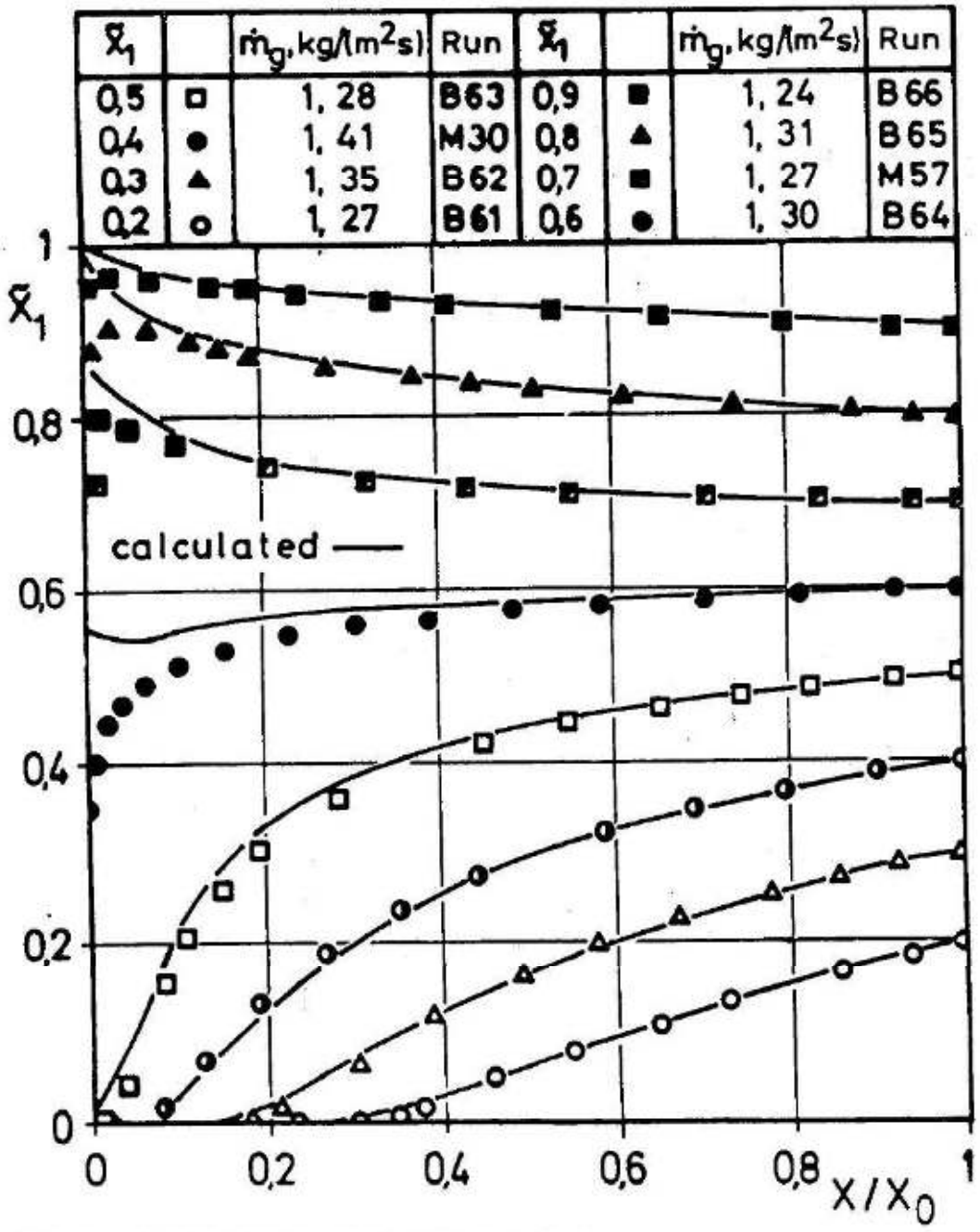

FIG. 3. CALCULATED AND EXPERIMENTALLY DETERMINED COMPOSITION CURVES

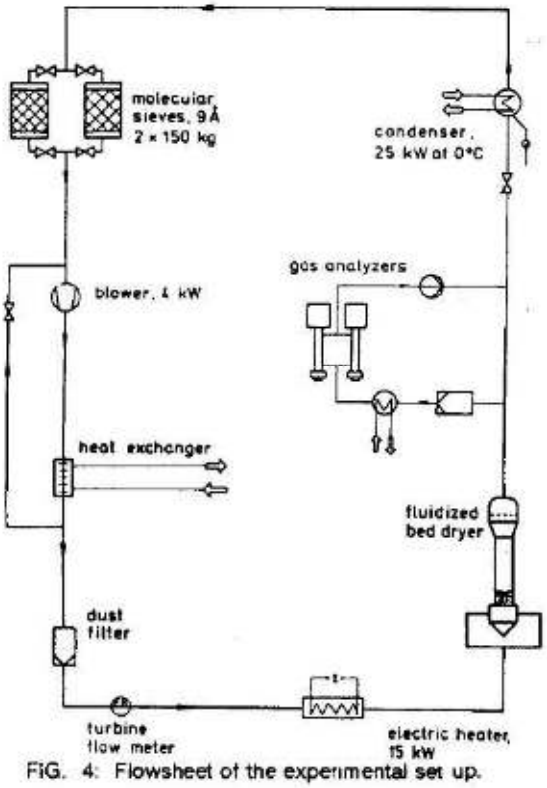

FIG. 4: Flowsheet of the experimental set up.

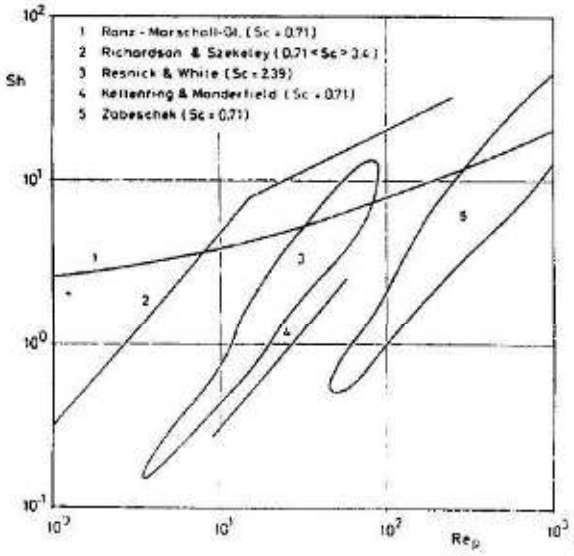

FIG. 5: Summary of some experimentally determined mass transfer coefficients.

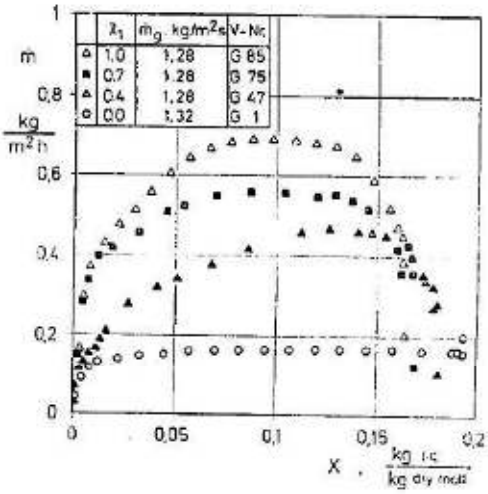

FIG. 6: Drying curves for different initial composition (Tw = 100oC; H = 15cm; dp = 1.35mm).

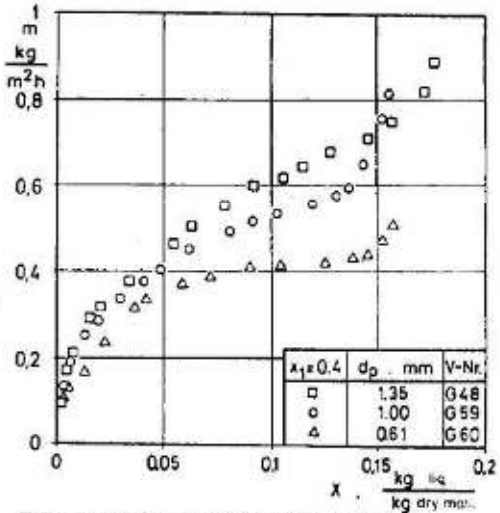

FIG. 7: Drying curves for different particle diameters (Two = 50oC; H = 10cm).

For heat transfer purposes thermal resistance due to the dry shell in small particles is negligible (6) leading to

$$NTU_t^{II} = NTU_t^{I} \qquad (16)$$

The specific evaporation flux from the surface of the particles is obtainable from mass balance:

$$\dot{n}_i = \frac{\dot{M}_g}{M_g A_b}\left[\tilde{Y}_{i,out} - \tilde{Y}_{i,in}\right] \qquad (16)$$

Combined with equation (8)

$$\dot{M}_i = \dot{M}_g \left[\tilde{Y}_i^* - \tilde{Y}_{i,out}^* \right] \left\{ 1 - e^{-NTU_i} \right\} \quad (17)$$

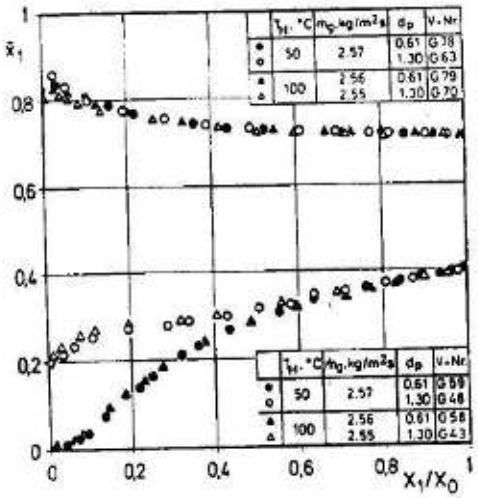

FIG. 8: Composition curves for different particle diameters and wall temperatures (H = 10cm).

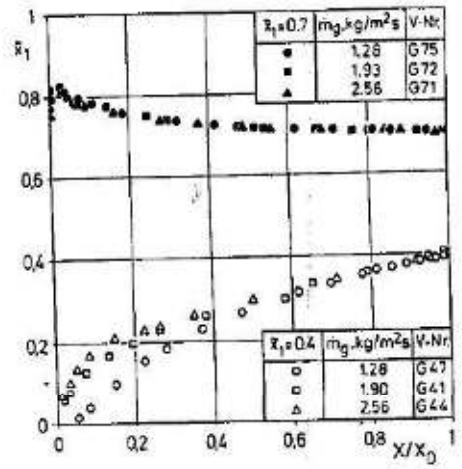

FIG. 9: Composition curves for different gas flow rate (Tw = 100oC; H = 15cm; dp = 1.35mm).

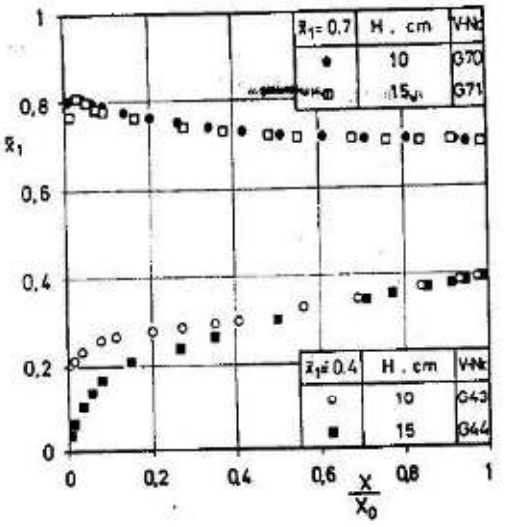

FIG. 10: Composition curves for different initial bed heights (Tw = 100oC; dp = 1.35mm).

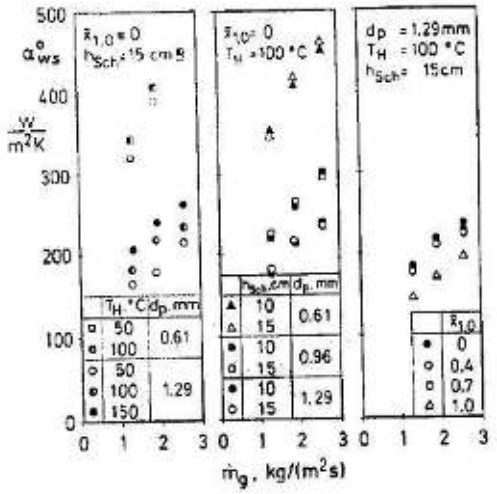

FIG. 11: Heat transfer coefficients.

2.4. Heat Transfer between Heated Wall and Fluidized Bed

The heat is transfered in three ways: by particle convection, gas convection and, at higher temperatures, radiation. The particle convection component is that part of the heat which is transmitted by conduction from the wall to the particles which make contact with it. The particles move into the

bulk of the bed and give up their surplus of internal energy. This mechanism is predominant with particles of less than 1mm radius (11).

The gas convection contribution is that part of the heat which goes directly from the wall to the gas in contact with it. This component increases with gas velocity and is therefore the biggest fraction in cases where larger particles, requiring higher velocities for fluidization, are concerned. The radiative component is, as usual, only of importance at higher temperatures.

Assuming a uniform bulk temperature the particle and gas convection components can be incorporated in a heat rate expression.

$$\dot{Q}_{wp} + \dot{Q}_{wg} = A_H \alpha_{WB} (T_w - T_B) \quad (18)$$

where α_{WB} is the wall-to-bed transfer coefficient. The heat balance can be expressed as:

$$\dot{Q} = \bar{H}_{out} - \bar{H}_{in} + \frac{d\bar{H}_B}{dt} \quad (19)$$

where $\bar{H}$ represents enthalpy. Thus equations (18) and (19) give

3. EXPERIMENTAL SET-UP AND RESULTS

3.1. Equipment Description

The nucleus of the set-up is a meter long copper tube with a diameter of 0.2m (fig.4). Its walls are electrically heated with heating mantles belted around it. Platinum 100 wires are imbedded at regular intervals along the wall to determine the temperature. A 4KW-blower connected to the bottom of the vertically-mounted tube supplies the required air flow. Between these two units is a turbine flow meter for flow rate determination. The exhaust gas from the top of the tube is filtered and partially condensed before entering a 9 Å NaX molecular sieve packed bed where its contents are reduced to zero. Part of the filtered air is bypassed through two infra-red devices which measure the concentration of the isopropanol and water in it. The solid material consists of aluminium silicate particles of density 1650kg/m3 and porosity of 30%. A table of the parameters studied and their values are given below.

Mole fraction of isopropanol:	0	0.4	0.7	1.0
Particle diameter (mm):		0.61	0.96	1.29
Bed height at rest (cm):		5	10	15
Gas flow rate (kg/m2s):		1.3	1.9	2.6
Wall temperature (oC):		50	100	150
Entry temperature of air (oC):		20		

3.2. Experimental Procedure

Weighed amounts of particles of a given height corresponding to a definite height, were wetted under vacuum with liquid of a certain concentration. The mixture of liquid and particles is centrifuged to make it fluidizable and then dumped into a hopper which opens into the copper tube. At the start of an experiment the blower, the condenser and the pump feeding the infra-red monitors are turned on. When the required operating conditions are attained, the recorders are started and the materials are simultaneously dumped into the tube. The experiment ends when both composition signals return to zero.

3.3. Results

The experimental results shown in figures 6 to 10 are plots of specific mass flux (kg/m^2s) against the moisture content (kg liquid/kg dry material), called the drying curve; and of mole fraction of isopropanol against the normalized moisture content, the composition curve.

Figure 6 indicates that the drying rate for pure isopropanol is about four times as much as that of pure water. The other curves show that higher rates are obtained for higher concentrations of alcohol. The higher volatility of isopropanol is responsible for this. It can also be observed that a period of pronounced constancy in drying rate is

obtained for the water. This is due to the ability of capillary forces to match the evaporative flux from the surface of the wet particles, given the lower water volatility. Measurements with single particles show that isopropanol exhibits no constant rate period at all. It falls right from the beginning of the drying period. The near constant rate observed here is a property of the total bed, since the effect of the increased resistance to diffusion is initially offset by the large surface area available.

Figures 7 to 10 indicate that temperature variation has very little effect on the selectivity, while that of particle size, bed height and velocity are appreciable. In fact the optimum condition for selectivity is achieved by a combination of small particles, high bed heights and low velocities at a given temperature. Since drying rates in small particles are lower than in large ones (fig.7), the combination given above consitute mild drying conditions. This is as opposed to the combination of large particles, low bed heights and high velocities, which gives severe drying conditions.

At the beginning of drying when the liquid forms a continuous phase in the pores and on the surface of the particles, mass transfer coefficients are highest. Therefore the NTUs are high (equation 14) resulting in the exit compositions being close to equilibrium. When the outer dried shell reduces the mass transfer coefficient and thus the NTU, the exit concentrations from the bed are far from equilibrium. In the limit the evaporative flux of component 1 is given by:

$$\dot{r} = \left[1 + \frac{D_{2,g}}{D_{1,g}} \frac{\tilde{Y}_2}{\tilde{Y}^*_1}\right]^{-1} \quad (21)$$

$$\left[D_{2,g} > D_{1,g}\right]$$

Which is less than that given by equation (8) i.e.

$$\dot{r} = \left[1 + \frac{\tilde{Y}_2}{\tilde{Y}^*_1}\right] \quad (22)$$

Figures 8 to 10 indicate that the biggest influence on selectivity is due to particle size. It has been determined that in large particles the transition from equation (21) to (22), represented on figure (2), is fast. Thurner and Schlunder (4) have shown that the selectivity observed in drying porous materials wetted with a mixture is due to more than just the resistance of the gas and the thermodynamic equilibrium at the drying front. A steep concentration profile, which does not reach the middle of the particle, is calculated for large particles. This is an indication of high liquid-side resistance to mass transfer. The mechanism can be related to the evaporation of a mixture from the surface of a porous slab which lies on the surface of the mixture. The kinetic mass transfer expression can be expressed as:

$$\dot{n}_1 = \dot{n}\,\tilde{x}_1 - n_1 K_1 \frac{d\tilde{x}_1}{dz} \quad (23)$$

which combined with equation (2) leads to

$$\frac{\dot{r}_1 - \tilde{x}_{1B}}{\dot{r}_1 - \tilde{x}^*_1} = \exp\left[-\frac{\dot{n}s}{n_1 K_1}\right] \quad (24)$$

Depending on the value of the liquid-side mass transfer coefficient K, two limiting cases exist.

1. For high K_ℓ; $\tilde{x}_{1B} = \tilde{x}^*_1$

It follows from equation (1) and figure (2) that the maximum selectivity will be obtained in this case. The concentration at the interface between the pore liquid and the surrounding gas, $\tilde{x}^*_1$ is equal to the bulk concentration. Thus the concentration profile has zero gradient.

2. For low K_ℓ; $\dot{r}_1 = \tilde{x}_{1B}$

This results in no selectivity at all, as can be inferred from equation (1).

It can be inferred from figure (2) that at low isopropanol concentrations the alcohol is removed while at concentrations lying above the dynamic azeotrope, water escapes preferably. The slight removal of the equilibrium curve from the diagonal at concentrations higher than the upper limit of the azeotrope 0.63, accounts for the low selectivity observed in this region. It can also be concluded that the selectivity trend found for

convective drying of the wet particles is the same as when the heat is transferred through the walls (6).

Figure (11) is a plot of the heat transfer coefficients calculated using equation (20). Due to the longer period of constant drying rate and bed temperature obtained using pure water, the first two diagrams of the figure are for water. These indicate that small particles, due to their larger surface area, give higher heat transfer coefficients. Higher wall temperatures give slightly high α-values attributable to the increasing importance of radiation and the increased thermal conductivity of the air.

The trend of high α-values at high gas throughputs is observed in all three diagrams. The larger heat transfer area resulting from the increased velocities is responsible. The third diagram shows that the α-values are, by and large, independent of the liquid composition. The lower values obtained for pure isopropanol cannot be explained.

SYMBOLS

A area	m^2
C_p specific heat capacity	kJ/kg.°C
D diffusivity	m^2
d_p mean particle diameter	m
H bed height	m
$\dot{H}$ enthalpy	kJ/kg mol
K mass transfer coefficient	m/s
$\dot{M}$ mass flux	kg/s
M molecular weight	-
N molar flux	mol/s
$\dot{n}$ ($\dot{m}$) specific molar (mass)flux	mol (kg)/m^2s
$\dot{Q}$ heat flux	m
r radius coordinate	m
$\dot{r}$ relative molar flux	-
R_p mean particle diameter	m
S selectivity	-
s slab thickness	m
t time	s
T temperature	°C
u velocity	m/s
$\tilde{x}$ liquid mole fraction	-
X moisture content on dry basis	-
$\tilde{y}$ gas mole fraction	-
Y mole ratio	-
α heat transfer coefficient	J/m^2Ks
ε porosity	-
μ tortuosity	-

Indices

b, B	bed
g	inert gas
i	component
w	wall
p	particle
ℓ	liquid
o	initial value
s	solid
1	isopropanol
2	water
~	molar
1.TA	first drying period
2.TA	second/falling-rate period
*	equilibrium

ACKNOWLEDGEMENT

This work was done at the Institute of Thermal Processes at the University of Karlsruhe, Karlsruhe, Federal Republic of Germany under the auspices of the International Seminar for Research and Teaching in Chemical Engineering and Physical Chemistry. Sincere gratitude is due the co-workers at the institute and the organisers of the Seminar.

LITERATURE CITED

1. Sklarenko S.I., M.K. Baranajew, Z. phys. Chem, Abt A, 175(1936) 195-202.

2. Sklarenko S.K., M.K. Baranajew, A. phys. Chem. Abt.A, 175(1936) 214-218.

3. Lewis W.K., L.Squires, Ind. Eng. Chem., 29 (1937) 109-114.

4. Thurner F., E.V. Schlunder, Proc. Third Int. Drying Symp., Birmingham, 1982 Drying International, Wolverhampton, Vol.2 pp 326-336.

5. Heiman F., E.V. Schlunder, To be published in Chem. Eng. Process (1988).

6. Schwarzbach J., E.V. Schlunder, To be published in Proc. 5th Int. Symp. Drying Versailles (1988).

7. Thurner F., E.V. Schlunder, Chem. Eng. Process, 20 (1986) 9-25.

8. Fitzgerald T.J., "Fluidization", 2nd Edition; J. Davidson, R. Clift, D. Harrison (1985)

9. Zabeschek G., Ph.D. Thesis, University of Karlsruhe (1977).

10 Schardler N., Ph.D Thesis, Technische Hochschule Darmstadt (1983).

11 Martin H., Chem. Eng. Process, 18 (1984) 157-169.

12 Resnick W., R.R. White, Chem. Eng. Process, 45 (1949) 377-390.

13 Richardson J.F., J. Szekely, Trans. Instn. Chem. Engrs. 39 (1961) 212-222.

14 Kettenring K.N., E. Mandersfield and J.M. Smith Chem. Eng. Prgr. 46 (1950) 139.

1)Areas suspected of arsenic and sulphur pollution near gold smelters, the ore being arsenopyrite;

2)Areas naturally containing large amounts of arsenic; and

3)Areas not containing much arsenic for control purposes.

Some characteristics of the soils selected for these studies are represented in Table 1.

The soils were air dried and screened to pass through 2mm openings. Their pH's were measured with a glass electrode on 1g portions shaken with 20cm^3 of O.O1M $CaCl_2$ solutions. Arsenate in the solutions was determined by the reduction distillation method of Small and McCants [11], phosphate by the ascorbic acid reduction method of Murphy and Riley [12], as modified by Harwood, Van Steenderen and Kuhn [13], and sulphate by the method of Chaudry and Cornfield [14].

Labile and surface phosphates were determined by the carrier [1] as well as carrier-free [15] methods.

In the carrier method 100 cm^3 of 10^{-4} M K_2HPO_4 solution of pH7 containing 1315 mBq of ^{32}P were added to 5g of soil Two drops of toluene were added to arrest any microbial activity and the contents were shaken for 24 hours at 25 ± O.5 °C. The solution was allowed to stand for 2 hours to settle and 25cm^3 of the suspension were centrifuged at 15,OOO r.p.m. for 3OOs. One cm^3 of the clear solution was evaporated to dryness on an aluminium planchet under an infra-red lamp and counted in a methane flow proportional counter.

Counts of the 5Oμ cm^3 of tagged K_2H PO_4 solution employed in shaking the soil was used as the standard.

In the carrier-free method, O.5g soil was shaken for 24 hours at a temperature of 25 ± O.5 °C in 1OOcm^3 of $1O^{-3}$ ammonium citrate buffer in $2X1O^{-2}$M KCl, the pH of which had been adjusted to the pH of the soil. The suspension was then tagged with 185mBq of carrier-free ^{32}P in1cm3 of solution and agitated for another 24 hours. Clear portions were obtained and analysed as before.

Labile and surface arsenate and sulphate were determined by the carrier-free method. In the arsenic determinations the suspension was tagged with 37mBq of carrier-free ^{74}As in 1cm^3 solution and 5cm^3 of the clear portions were used for counting on a Nuclear Enterprises NaI (TL) scintillation counter. The amount of ^{74}As added was estimated by adding the same amount of ^{74}As to three flasks containing 1OOcm^3 of the citrate-KCL buffer and 5, 10, 15 μg arsenic as KH_2AsO_4. The ϰ -count in these could be reproduced on the same instrument as that used for the soil extracts to within the allowable statistical error of counting. In the labile and surface sulphate determinations, the soil suspensions were tagged with562 μBq of carrier-free ^{35}S in 1OO dm^3 of solution. One cm^3 of the clear sample solution was mixed with diphenyl oxazole and counted on a Packard liquid scintillation counter. A standard count was made by the adding 1OO μdm^3 of carrier-free ^{35}S to three flasks containing 1OOcm^3 of the citrate-KCl buffer and 5, 1O, 15 ug of sulphur as $CaSO_4.2H_2O$. In all cases the clear filtrates were analysed for ions as al-

TABLE 1: TOTAL PHOSPHATES, ARSENATE AND PH OF SOILS.

	No. of Samples	Range	Mean	Standard deviation	Coefficient of variation
Total-P	30	86-1683 ($mgkg^{-1}$)	411($mgkg^{-1}$)	348($mgkg^{-1}$)	79
Total-As	30	2-157($mgkg^{-1}$)	48($mgkg^{-1}$)	43($mgkg^{-1}$)	89
pH	36	3.10-6.60	5.11	1.81	35

TABLE 2: AVAILABLE PHOSPHATE BY CHEMICAL EXTRACTANTS.

	No. of Samples	Range ($mgkg^{-1}$)	Mean ($mgkg^{-1}$)	Standard deviation	Coefficient of variation
EDTA-P	35	6-628	161	205 ($mgkg^{-1}$)	127(%)
NaOH-P	31	7-453	102	105	103
Bray-P_1	34	< 1-838	71	194	273
Bray-P_2	36	1-331	45	79	176
Bray-P_3	15	18-556	208	310	101
Olsen	20	3-440	87	96	110
Truog	36	2-172	26	40	154

TABLE 3: LABILE (L) AND SURFACE (S) IONS.

Carrier Method	No. of Samples	Range ($mgkg^{-1}$)	Mean ($mgkg^{-1}$)	Standard deviation	Coefficient of variation
L_p	36	2-1989	268	420	157
S_p	33	< 1-804	254	11	434
Carrier free Method					
Lp	36	2-1315	115	224	195
LAs	17	< 1-12	3	3	100
Ls	22	< 1-604	293	136	46
Sp	36	1-1272	191	235	123
SAs	11	< 1-4	2	2	100
Ss	22	3-192	80	50	63

TABLE 4: CORRELATION BETWEEN SURFACE PHOSPHOROUS AND OTHER PHOSPHOROUS VALUES.

INDEPENDENT VARIABLE (x)	Degrees of Freedom	Correlation coefficient	Regression equation
	DEPENDENT VARIABLE, CARRIER Sp (Y)		
1. EDTA-P	31	0.6223	Y= 3.4077 + 0.5709x
2. Bray-P1	31	0.6982	Y= 39.8218 + 0.6711x
3. Bray-P2	31	0.6935	Y= 186.46 83 + 9.6225x
4. Truog-P	31	0.7929	Y = 10.531 3 + 3.6480x
5. Bray-P4	12	0.7890	Y= 96.8058 + 0.6474x
6. Olsen-P	17	0.5525*	Y= 56.1210 + 0.2297x
7. Total-P	26	0.7094	Y= 65.3127 + 0.3735x
8. Carrier-free Sp	31	0.6981	Y= 10.5003 + 0.6378x
	DEPENDENT VARIABLE, CARRIER-FREE Sp (Y)		
9. Bray-P1	31	0.6568	Y= 127.8449 + 7314x
10. EDTA-P	31	0.4581#	Y= 106.5595 + 0.494x
11. Bray-P2	31	0.6490	Y= 104.2610 + 0.9413x
12. Truog-P	31	0.6102	Y= 97.7526 + 0.6613x
13. Bray-P4	12	0.6134*	Y= 58.1656 + 0.8841x
14. Total-P	27	0.7521	Y= 8.1667 + 0.4623x

*Significant at less than 0.02 level #Significant at less than 0.01 level
The other values are significant at less than 0.001 level.

ready indicated and "Surface ion" calculated by these equations:

Carrier Method: Surface ion =

$$\left[\frac{(\text{Specific Activity})_i}{(\text{Specific Activity})_f \text{ solution}} - 1\right] \times (\text{Ion concentration})_i$$

Carrier-free method: Surface ion =

$$\left[\frac{(\text{Isotopic ion in solution})_i}{(\text{Isotopic Ion in solution})_f} - 1\right] \times (\text{Ion Concentration})$$

The suffixes i and f in the above equations refer to initial and final respectively.

Labile ion by either method equals the sum of surface ion and ion concentration of the filtrate.

CHEMICAL EXTRACTANTS

The following methods were employed

(a) EDTA-P, the method of Alexander and Robertson, [16] as modified by Amonoo-Neizer and Azuma [17];

(b) NaOH-P, 0.1MHNaOH + 0.1MNaCl;

(c) Bray-P_1, 0.03M NH_4F + 0.1M HCl;

(d) Bray-P_2, 0.03MNH_4F + 0.1MHCl;

(e) Bray-P_4, 0.5M NH_4F + 0.1M NHl;

(f) Olsen, 0.5M $NaHCO_3$ at pH 8.5; and

(g) Truog, 0.001MH_2SO_4 in 3% $(NH_4)_2SO_4$.

RESULTS AND DISCUSSION

The total phosphorus values were generally higher than have been previously obtained [18]. Total arsenic values on the other hand were lower than have been obtained elsewhere [19] but are comparable to values obtained in some other contaminated soils [20]. The pH of the soils range between 3.10 and 6.60. The more acidic ones are located near gold smelters where lots of sulphur and arsenic find their way into the soil as soluble acidic oxides thus accounting for their low pH.

Other results are shown in tables 2,3,4. The carrier method was more suitable when the water soluble phosphate content of the soil was low whilst the carrier-free method was superior in situations where the soil contained large amounts of phosphate. Labile and surface arsenate and sulphate were determined by the carrier-free method because most of the areas where knowledge of labile and surface arsenate and sulphate was of interest had substantial amounts of water soluble arsenate. The results obtained by the carrier and carrier-free methods, Table 3, for the phosphate experiments were generally higher when determined by the carrier method than when determined by the carrier-free method. No such general trend was observed with surface phosphate as determined by the two methods. The figures obtained for labile and surface phosphate for any particular soil were much nearer in value, using carrier-free method than with the carrier method. Labile and surface arsenate range from less than 1 to 12 and less than 1 to 4mgkg^{-1} whilst those for sulphate range from less than 1 - 604 and 3 to 192mgkg^{-1} respectively. The fact that the sulphate was more readily exchangeable than arsenate may be due to arsenate being more strongly fixed than sulphate. Most of the readily exchangeable sulphate and arsenate occurred in the polluted soils.

Correlation analyses, Table 4, show that surface phosphate as determined by the two methods were highly related to available phosphorus as determined by chemical extractants, total-P, and also to each other. The probability of correlation being accidental was less than 0.001 in every case except for those between carrier phosphate and Olsen-P, with a probability of 0.02, carrier-free phosphate and EDTA-P, 0.01, and carrier-free phosphate and Bray-P4, 0.02. Both carrier and carrier-free surface phosphate did not correlate with NaOH-P.

Since surface phosphate values correlate so well with all the values obtained by using the chemical extractants for determining available phosphorus, except for NaOH-P, it may prove a more useful, quicker and convenient method of determining available phosphate in any particular case where any such chemical extractant has proved applicable, as judged by uptake by plants.

REFERENCES

1. TALIBUDEEN, O. Isotopically exchangeable phosphorus in soils, J. Soil Sci. Vol. 1 pp 120 - 129, 1956.
2. OLSEN, S.R. Inorganic phosphorus in alkaline and Calcareous soils in PIERE, W.H. & NORMAN, A.G., ed. Soil and Fertilizer Phosphorus in Crop Nutrition, New York, Academic Press Inc. Vol. IV, pp89-123, 1958.
3. GUNNARSSON, O. & FREDRIKSSON, L. Radioisotope techniques, London, Her Majesty's Stationery Office, Vol. 1, pp 427, 1958.
4. McAULFEE, C.D., HALL, N.S. DEAN, L.A. & HENDRICKS, S.B., Exchange reaction between phosphates and soils. Hydroxylic surfaces of soil minerals, Proc. Soil Sci. Soc. Am. Vol. 12, pp

S.N., Isotopic equilibria between phosphates in soils and their significance in the assessment of fertility by tracer methods, J. Soil Sci. Vol. 5, pp 85 - 105, 1954.
6. WILKLANDER, J. Lantbr. Hogst. Annlr. Vol. 17, pp 407, 1950.
7. TALIBUDEEN, O. The determination of isotopically exchangeable phosphorus in some Rothamsted soils, Proceedings of Radioisotope Conference pp 405 - 411, 1954.
8. COPPER, H.P., PADEN, W.R., HALL, E.E., ALBERT, W.B. ROBERS, W.B. & PILEY, J.A. Effect of calcium arsenate on the productivity of certain soil types. South Carolina Agric. Exp. Stn. Rep. Nos. 28 - 37, 1931.
9. MacPHEE, A.W., CHISHOLM, D., & MacEACHERN, The persistence of certain pesticides in the soil and their effect on crop fields. Can. J. Soil Sci., Vol. 40, pp 59 - 62, 1960.
10. Jones, J.S. and Hatch, M.B., The significance of inorganic spray residue accumulation in orchard soils. Soil sci. Vol. 44, pp 37-53, 1937.
11. SMALL, A.G. J.R., & Mc CANTS, G.B., Determination of arsenic in flue cured tobacco and in soils, Proc. Soil Sci. Am. Vol. 27, pp 348-348, 1962.
12. MURPHY, J. & RILEY, J.P., A modified single solution method for the determination of soluble phosphates in natural waters. Analytical Chem. Acta, Vol. 27, pp 31-36, 1962.
13. HARWOOD, J.E., VAN STEENDEREM, R.A. & KURN, A.L., A rapid method for phosphate analysis at high concentration in water, Water Research, Vol. 3, pp 417-423, 1966.
14. CHAUDRY, J.S. & CORNFIELD, A.H., The determination of total sulphur in soil and plant material. Analyst Lond; Vol. 91, pp 528-530, 1966.
15. OLSEN S.R. Measurement of surface

with radioisotope phosphorus. J. Phys. Chem. Vol. 56, pp 630-632, 1952
16. ALEXANDER, T.G. & ROBERTSON, J.A. EDTA extractable phosphorus in relation to available and inorganic phosphorus forms in soils. Soil Sci., Vol. 114, No. 1, pp 69-72, 1972.
17. AMONOO-NEIZER, E.H. & AZUMAH, J.S., Relationship between ethylenediamine-tetraacetic acid extractable phosphorus and inorganic phosphorus. Ghana J. Sci. Vol. 17, No. 1, p 121-124, 1979.
18. HALM, A. T. AND BAMFOE-ADDO, A. Available phosphorus as related to inorganic phosphate fractions in some Ghana soil series, Ghana J. Sci. Vol. 5, pp 89-94, 1972.
19. WOOLSON, E. A., AXLEY, J. H. & KEARNEY, P. C., The chemstry and phototoxicity of arsenic in soils 1. Contaminated filed soils. Proc. Soil Sci. Am. Vol. 35, pp 938-943, 1971.
20. CRECELIUS, E.A., JOHNSON, C. J. AND HOFER, G. C., contamination of soils near a copper smelter by arsenic, antimony and lead. Water Air and Soil Pollution, Vol. 3, pp 337-342, 1974.